

Cite this: *RSC Adv.*, 2014, 4, 37812Received 8th May 2014
Accepted 1st August 2014

DOI: 10.1039/c4ra07541b

www.rsc.org/advances

The astonishing progress in performance of hydrogel triggered by the structure evolution of cross-linking junctions†

Pengchong Li,^{ab} Kun Xu,^{*a} Ying Tan,^a Cuige Lu,^{ab} Yangling Li,^{ab} Haiwei Wang,^{ab}
Xuechen Liang^{ab} and Pixin Wang^{*a}

Novel microgel composite hydrogels characterized with the structural evolution of crosslinking junctions were prepared. Under the pH stimulus, the high-strength hydrogels exhibit a drastic and sudden volume phase transition, which derives from the dissociation and association of crosslinks.

Smart hydrogels have been applied extensively in the area of soft-wet devices and biomaterials because of their unique three-dimensional network structure, stimuli-responsiveness, flexibility, high liquid content and good biocompatibility.^{1–3} Among the several characteristics of smart hydrogel, nonlinear response makes them unique and effective. Significant changes in the hydrogel structure and properties can be caused by external small stimulus.

Up to now, the responsiveness of most hydrogels relies on the inherent nature of the functional groups of polymer chains of its network. Endowing a hydrogel with smart responsiveness is challenging with the prevalent investigation and design of soft-wet materials.⁴ However, the relaxation and heterogeneity of the cross-linking network heavily retard the response rate of bulk hydrogel materials toward environmental stimuli. Although several strategies, including introducing porosity,⁵ altering the micro-scale⁶ and homogeneity of the cross-linking network,⁷ during the fabrication of hydrogel materials have been explored to improve this drawback. However, despite this a revolutionary and creative idea is still anticipated for fabricating perfect hydrogel materials with a fast response rate. The structure and properties of cross-linking junctions are crucial to fabricate a 3D network and it has been extensively used to regulate the mechanical performance of hydrogels, such as a

topological hydrogel with a sliding figure-of-eight cross-linking ring,⁸ a tetra-arms polymer hydrogel,⁹ a nanocomposite hydrogel with clay layer cross-linking agent,¹⁰ a physically cross-linked hydrogel based on various physical interactions¹¹ and macro-sphere composite hydrogels.¹² Although the mechanical performance of these hydrogels can be significantly improved because of the presence of special cross-linking structures, their responsive properties still depend on the inherent nature of functional groups in their network.

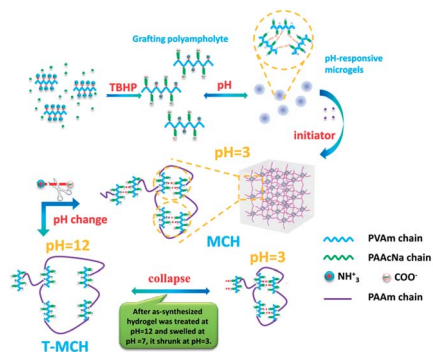
In our preliminary studies,^{13,14} a series of novel composite hydrogels with a responsive microgel as initiator and cross-linking points have been synthesized, in which smart cross-linking sites can endow a non-responsive hydrogel matrix with a unique smartness. Herein, to pursue a new method for repairing the disadvantages of hydrogel (slow response rate and poor mechanical strength), we rely on the stimuli-controlled cross-linking junctions to fabricate novel hydrogel materials that creatively utilize cross-linker points for structural evolution and interaction according to environmental stimuli to regulate their responsiveness. As a consequence, smart cross-linking junctions endow non-responsive hydrogel matrix with unique responsiveness, and the characteristic manifestation of the deswelling dynamic of our hydrogel is completely different from those of the conventional hydrogels.

First, polyvinylamine-graft-polyacrylate sodium (PVAm-g-PAAcNa) grafting polyampholytes are prepared by grafting PAAcNa chains onto PVAm backbone using the oxidation-reduction reaction between the primary amine groups of PVAm and *tert*-butyl hydroperoxide (TBHP), as reported previously.¹⁵ Over an appreciable pH range, the microgels can spontaneously form due to static-electrolytic complexation. As shown in Fig. S1,† it is suggested that microgels have good dimensional homogeneity. The fabrication method reported in our previous works,^{13,14} involving the oxidation-reduction reaction between the primary amine groups of microgels and TBHP is utilized again to synthesize MCH by connecting the microgels with grafting PAAm chains on the surface of microgels (as shown in Scheme 1).

^aKey Laboratory of Polymer Ecomaterials, Changchun Institute of Applied Chemistry, Chinese Academy of Sciences, Changchun, China. E-mail: pxwang@ciac.ac.cn; xukun@ciac.ac.cn

^bUniversity of Chinese Academy of Sciences, Beijing, China

† Electronic supplementary information (ESI) available: Syntheses and characterization of microgels and hydrogels; supplementary figures and table. See DOI: 10.1039/c4ra07541b



Scheme 1 The proposed synthesis and structural evolution mechanism of MCH.

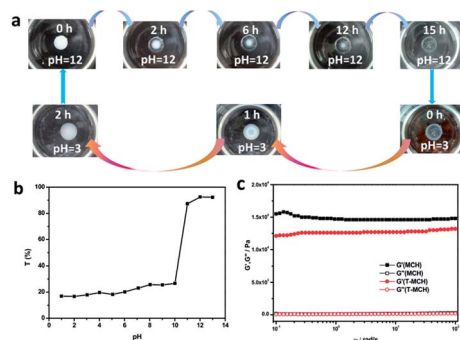


Fig. 1 (a) The evolution of MCH appearance under external pH stimuli. (b) The transmittance of MCH vs. environmental pH. (c) The rheological measurement of MCH and T-MCH.

It should be noted that microgels, as cross-linking junctions, possess pH-responsiveness, which can disassociate into grafting polyampholytes at pH > 12. Thus, the structure of the as-prepared MCH exhibits change that corresponds to an external stimuli response. As shown in Fig. 1a, the as-synthesized MCH sample (with 15 mm diameter and 25 mm height) is white and opaque, and it becomes transparent after it is soaked into an alkali solution (pH = 12) within 15 h. When the alkali-treated MCH sample is again transferred into an acid solution (pH = 3), it rapidly becomes opaque and white within 2 h with slight shrinking. Comparing the two processes, the rate of transformation from transparency to opaqueness is faster than that of the reverse procedure. This suggests that the structure of MCH can exhibit a certain reversible transition under pH stimulus and that this transition is governed by more than the diffusion of the solvent medium.¹⁶ In this paper, the transparent hydrogel after alkali treatment is denoted as T-MCH. It is prepared by soaking MCH into an alkali solution (pH = 12) for a certain time interval until the hydrogel changes from opaque to transparent and the time interval rests with the size and shape of the hydrogel. Meanwhile, we know from Fig. 1b that the optical transmittance of MCH is about 20–30%, ranging from pH = 1 to 10 and abruptly jumps to more than 90% at pH > 12.

Meanwhile, the rheological measurement is also used to analyze the structural evolution of MCH and T-MCH under environmental pH stimuli, and the result suggests that the

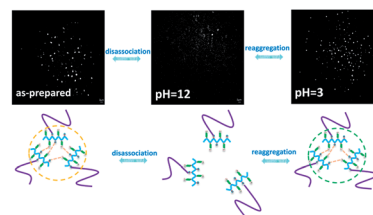


Fig. 2 The structural evolution of microgel cross-linking junctions in MCH according to the change of external pH (the bar is 2 μm).

elastic modulus of T-MCH is lower than that of MCH (see Fig. 1c). Calculated according to eqn (1):¹⁷

$$G_e = NRT \quad (1)$$

where G_e is the plateau modulus from the G' vs. ω curves in the low frequency range. R and T are the gas constant and absolute temperature, respectively.

The effective cross-linking density of T-MCH is 4.631 mol m⁻³, which is smaller than that of MCH (6.027 mol m⁻³). This result suggests that the cross-linking network becomes loose under higher pH conditions (pH > 12).

Herein, the measurement of super-resolution fluorescence microscopy is carried out to elucidate the structural evolution of microgel cross-linking junctions into a composite hydrogel when environmental pH is adjusted. The fluorescent dye (Alexa Fluor @647) was employed because of its ability to selectively bind between primary amine groups and fluorescent dye.¹⁸ As shown in Fig. 2, for the as-synthesized MCH, the fluorescent photograph shows large amount of aggregating domains with 0.3–1.5 μm dispersed into the entire endoscope. This suggests that the cross-linking points exist in the form of microgels and their aggregation state instead of disassociating grafting polyampholyte. However, after MCH was treated in alkali solution and became T-MCH, the aggregating domains almost disappeared. Instead, several fluorescent points are evenly dispersed into the entire endoscope, and the response is a completely transparent hydrogel. Moreover, after transparent T-MCH restores to opaque MCH in acidic solution (pH = 3), the aggregation of fluorescent domains occur again. This result demonstrates that reversible structural evolution of microgel cross-linking junctions induced by the change in environmental pH (as discussed in Fig. S2†) can endow a unique smartness into a hydrogel material.

As shown in Fig. 3, the maximum shrinking percentage of NMBA-H is only 63.8%, and its shrinking rate is very slow in aqueous solution with a time required to obtain maximum shrinking ratio of more than 2100 min. For T-MCH, the maximum shrinking percentage can be up to 98.5% due to structural evolution of microgel cross-linking junctions. Meanwhile, the time required to reach a 50, 75 and 90% shrinking percentage is 0.65, 2 and 5 min, which are 18, 30 and 400 times faster, respectively, than those of NMBA-H. In general, the non-ionic PAAm hydrogel is insensitive to the weak acid environment because of the absence of ionic groups in its structure.¹⁹ Thus, the collapse of NMBA-H in Fig. 3a may come

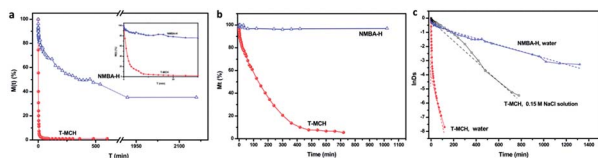


Fig. 3 The shrinking dynamic curves of T-MCH and NMBA-H in (a) aqueous and (b) 0.15 M NaCl solution. (c) The treatment of curves to acquire the characteristic time.

from the change in ionic strength according to various pH levels tested. In Fig. 3b, the de-swelling dynamics of samples in 0.15 M NaCl solution is investigated. The result demonstrates that the maximum shrinking ratio of T-MCH is *ca.* 95% and the time required to reach 50, 75 and 90% shrinking ratio is 105, 240 and 420 min, respectively, whereas the swelling ratio of NMBA-H remained constant.

For the de-swelling kinetics in stimuli-responsive hydrogels, Tanaka²⁰ and Ogawa²¹ pointed out that the characteristic time (τ) for shrinking was given by:

$$e^{-\left(\frac{t}{\tau}\right)} \approx \frac{M_t - M_e^c}{M_e^s - M_e^c} \quad (2)$$

where M_e^s and M_e^c represent the equilibrium swelling ratio of the swollen and the collapsed state, respectively.

From the fitting curves and the dynamic parameters of various samples, as shown in Fig. 3c and Table S1,[†] we can find that all the samples possess two-stage fitted dynamic curves with different τ . In the first stage, the τ_1 of T-MCH is 2.76 min, which is slightly smaller than those of NMBA-H (4.38 min). However, an obvious difference is noted that the first stage with τ_1 being the principal part of the de-swelling dynamic of T-MCH. When it ends, T-MCH collapses to more than 90% under de-swelling, which is clearly different from the shrinking dynamic behavior of conventional hydrogels. For NMBA-H, the first stage of τ_1 is very short and only accounts for 10–15% of the total de-swelling. This result elaborates on the idea that a skin layer forms following the first stage, which impedes water molecule to escape from the interior of the hydrogel network.²² The second stage, τ_2 is an important segment of their shrinking dynamics, and the τ_2 value for NMBA-H is 413.22 min, which is far more than that of T-MCH (25.94 min). As far as T-MCH is concerned, although microgel cross-linking junctions disassociate into grafting copolymers during alkali treatment, the chemical bonds between PAAm chains and primary amine groups of microgels still are well maintained. Thus, the dense, heterogeneous cross-linking structure of MCH is translated into the loose, homogeneous cross-linking structure of T-MCH. Most importantly, there are large amounts of flexible ampholytic polymer chains bearing various signs, as the legs of a myriapod, which are formed because of the disassociation of microgels on the network structure of T-MCH. When swollen T-MCH in distilled water is transferred into an acidic solution (pH = 3), the flexible, hydrophilic grafting polymer chains, as the legs of myriapod, exhibit excellent mobility and act as releasing channels for water molecules within the skin layer, preventing a

reduction in the shrinking rate. At the same time, the charges of grafting copolymers can reform ion-pairs and help create releasing channels for water molecules in the skin layer, which can accelerate the shrinking of T-MCH network during collapse. Thus, the improvement in the response rate of T-MCH is astonishing.^{23,24}

However, as shown in Fig. 3c and Table S1,[†] the de-swelling behaviors and character parameters of T-MCH in salt solution exhibit obvious differences. The first stage with τ_1 is very short and only from 15–20% of the total de-swelling. The τ_1 and τ_2 values are 22.78 and 144.51 min, respectively, which are far more than those of the samples in distilled water. As to the reason that the de-swelling response rate of T-MCH obvious turns slow in 0.15 M NaCl solution compared with that in aqueous solution, we attribute this to the formation of ion-pairs that can be disturbed by salt when T-MCH collapses in salt solution.

In summary, the structural evolution of stimuli-controlled cross-linking junctions is creatively employed to regulate the structure and performance of a composite hydrogel and significant progress in soft-wet materials was obtained. Herein, the smartness of cross-linking points can endow a hydrogel material with unique stimuli-responsiveness. At the same time, the response rate and mechanical strength of hydrogel materials can be improved. The attempt reported here can open a new avenue in the research of hydrogel materials.

Acknowledgements

This work was financially supported by the National Natural Science Foundation of China (grant nos 51321062 and 51103150).

Notes and references

- 1 R. A. Stile, W. R. Burghardt and K. E. Healy, *Macromolecules*, 1999, **32**, 7370–7379.
- 2 G. Pan, Q. Guo, Y. Ma, H. Yang and B. Li, *Angew. Chem.*, 2013, **125**, 7045–7049.
- 3 E. A. Appel, X. J. Loh, S. T. Jones, F. Biedermann, C. A. Dreiss and O. A. Scherman, *J. Am. Chem. Soc.*, 2012, **134**, 11767–11773.
- 4 M. R. Islam, X. Li, K. Smyth and M. J. Serpe, *Angew. Chem.*, 2013, **52**, 10330–10333.
- 5 J.-T. Zhang, S.-X. Cheng, S.-W. Huang and R.-X. Zhuo, *Macromol. Rapid Commun.*, 2003, **24**, 447–451.
- 6 E. C. Cho, J.-W. Kim, A. Fernández-Nieves and D. A. Weitz, *Nano Lett.*, 2007, **8**, 168–172.
- 7 Y. Tan, K. Xu, P. Wang, W. Li, S. Sun and L. Dong, *Soft Matter*, 2010, **6**, 1467–1471.
- 8 G. Fleury, G. Schlatter, C. Brochon, C. Travelet, A. Lapp, P. Lindner and G. Hadzioannou, *Macromolecules*, 2007, **40**, 535–543.
- 9 T. Sakai, Y. Akagi, T. Matsunaga, M. Kurakazu, U.-i. Chung and M. Shibayama, *Macromol. Rapid Commun.*, 2010, **31**, 1954–1959.

- 10 K. Haraguchi and T. Takehisa, *Adv. Mater.*, 2002, **14**, 1120–1124.
- 11 W. Li, H. An, Y. Tan, C. Lu, C. Liu, P. Li, K. Xu and P. Wang, *Soft Matter*, 2012, **8**, 5078–5086.
- 12 T. Huang, H. G. Xu, K. X. Jiao, L. P. Zhu, H. R. Brown and H. L. Wang, *Adv. Mater.*, 2007, **19**, 1622–1626.
- 13 P. Li, K. Xu, Y. Tan, C. Lu, Y. Li and P. Wang, *Polymer*, 2013, **54**, 5830–5838.
- 14 K. Xu, Y. Tan, Q. Chen, H. An, W. Li, L. Dong and P. Wang, *J. Colloid Interface Sci.*, 2010, **345**, 360–368.
- 15 P. Li, J. Zhu, P. Sunintaboon and F. W. Harris, *Langmuir*, 2002, **18**, 8641–8646.
- 16 B. Amsden, *Macromolecules*, 1998, **31**, 8382–8395.
- 17 L. Xiong, M. Zhu, X. Hu, X. Liu and Z. Tong, *Macromolecules*, 2009, **42**, 3811–3817.
- 18 C. Flors, *J. Microsc.*, 2013, **251**, 1–4.
- 19 M. Sivanantham, R. Kesavamoorthy, T. N. Sairam, K. N. Sabharwal and B. Raj, *J. Polym. Sci., Part B: Polym. Phys.*, 2008, **46**, 710–720.
- 20 T. Tanaka, E. Sato, Y. Hirokawa, S. Hirotsu and J. Peetermans, *Phys. Rev. Lett.*, 1985, **55**, 2455–2458.
- 21 Y. Ogawa, K. Ogawa and E. Kokufuta, *Langmuir*, 2004, **20**, 2546–2552.
- 22 Y. Kaneko, R. Yoshida, K. Sakai, Y. Sakurai and T. Okano, *J. Membr. Sci.*, 1995, **101**, 13–22.
- 23 R. Yoshida, K. Uchida, Y. Kaneko, K. Sakai, A. Kikuchi, Y. Sakurai and T. Okano, *Nature*, 1995, **374**, 240–242.
- 24 Y. Kaneko, S. Nakamura, K. Sakai, T. Aoyagi, A. Kikuchi, Y. Sakurai and T. Okano, *Macromolecules*, 1998, **31**, 6099–6105.